

LINE IDENTIFICATIONS OF TYPE I SUPERNOVA SPECTRA REVISITED: DETECTIONS OF UNBURNED HYDROGEN IN TYPE IB, IC, AND MORE LUMINOUS EVENTS

J. T. PARRENT¹, D. MILISAVLJEVIC¹, A. M. SODERBERG¹, M. PARTHASARATHY²

Draft version June 28, 2022

ABSTRACT

The spectrum of a supernova results from a complex array of overlapping atomic signatures that are sensitive to the composition and state of unburned and freshly synthesized material. Most theoretical models indicate that observed features near 6000 – 6300 Å in type I spectra are due to more than a single component of Si II λ 6355, if at all for poorly matched Ibc and super-luminous supernovae; an interpretation of Si II λ 6355 works for nominal 6150 Å absorption features of all type Ia supernovae during the first month of free expansion while the same interpretation has not been successful for a majority of type Ibc. Instead, canonical 6250 Å absorption features of type Ibc spectra are likely shaped primarily by faint signatures of H α . Meanwhile, we also find the identification of Si II λ 6355 in the spectra of broad-lined Ic and super-luminous events of type I/R is less convincing in spite of numerous model spectra used to show otherwise. Here we argue a more likely explanation for these 6000 – 6300 Å features is that they are conspicuous signatures of blue-shifted absorption and emission in H α , which is frequently observed in the spectra of hydrogen-rich, type II supernovae. Such a solution has yet to be investigated in detail for classically defined type I supernovae on account of historical mix-ups in supernova nomenclatures; type I means no hydrogen [sic]. Here we revisit line identifications of type I supernovae and highlight unburned hydrogen as an important free parameter.

Keywords: supernovae: general — supernovae: individual (SN 1954A, 1984L, 1987K, 1987M, 1990B, 1990I, 1991T, 1991bg, 1993J, 1994D, 1994I, 1996cb, 1997ef, 1998bw, 1999aa, 1999dn, 2002ap, 2002bj, 2002bo, 2002cx, 2002es, 2003dh, 2003lw, 2005cs, 2005ek, 2005hk, 2006gz, 2006jc, 2007bi, 2007gr, 2008D, 2009jf, 2010X, 2010ah, 2011fe, 2012ap, 2012hn, and LSQ12dlf)

1. INTRODUCTION

In terms of taxonomy, or a spectral sequence, supernovae of various luminosity classes are divided into two central categories, types I and II, depending on whether or not the spectrum contains conspicuous signatures of hydrogen (Minkowski 1941). For type II supernovae (SN II), signatures of hydrogen Balmer lines come in the form of distinct P Cygni profiles. Depending on the decline in the light curve, type II supernovae can be further sub-classified as SN IIL for a linear decline and SN IIP for sustained brightness before an eventual decline. However, drawing distinctions between SN IIL and IIP is less obvious considering an existing continuum of observed properties (Sanders et al. 2014; Faran et al. 2014; Pejcha & Prieto 2015; Gall et al. 2015).

Broadly speaking, hydrogen-poor SN I supernovae are separated into three subclasses, SN Ia, Ib, and Ic. The spectra of thermonuclear SN Ia reveal conspicuous signatures of Si II λ 6355, while the latter varieties of SN I core-collapse supernovae do not (Filippenko 1997). Instead, SN Ibc classes signify the presence of weak signatures of hydrogen and helium. Meanwhile, the spectra of some SN Iib start out as SN II in appearance, with weak H α , but later transition to a spectrum with lines of helium similar to SN Ib (Filippenko 1988, see Wheeler et al. 1995 for a review).

A precise definition of SN Ibc from interpretations of select spectral features has since varied over the years (see Fryer 2004; Gray & Corbally 2009). Some interpretations assume no hydrogen can be found in a type I spectrum, while lone detections of Si II λ 6355 are deemed robust for SN Ibc (see Taubenberger et al. 2006; Hachinger et al. 2012).

As noted above, stripped-envelope subclasses of SN Ibc are defined as not having a doublet signature of Si II λ 6355, which is a line detected for all SN Ia. However, in Fig. 1 of Filippenko (1997), weak absorption features near 6250 Å are labeled as Si II for both SN Ib 1984L and SN Ic 1987M, leading the reader to suspect SN Ibc spectra harbor weak features of silicon, when indeed the feature may be faint detections of unburned hydrogen (see our Figure 1).

Nevertheless, one argument disfavoring detections of faint H α in the spectra of SN Ibc is that identification of H α is led astray by discordant measurements of blended absorption minima, e.g. as can be obtained with semi-empirical tools like SYNAPPS. This is incorrect; interpretational discrepancies exist between H I λ 6563 and Si II λ 6355 given the proximity of rest wavelengths and the degree to which the associated blended absorption components are blue-shifted. Yet SYNAPPS has been used to identify Si II λ 6355 in a number of SN Ibc, as well as more luminous events, when the model spectra provided are incompatible with observations.

A misidentification of Si II for SN Ibc can be recognized when signatures of Si II and Fe II indicate layers of Si II are well below opaque layers of Fe II

¹ Harvard-Smithsonian Center for Astrophysics, 60 Garden St., Cambridge, MA 02138, USA

² Indian Institute of Astrophysics, Koramangala, Bangalore, 560034, India

(Stathakis et al. 2000). Small displacements in line velocities ($\lesssim 1500 \text{ km s}^{-1}$) are not unheard of for SN Ia since the spectrum transitions to a phase where lines of Fe II are relatively more indicative of regions of bulk line formation than Si II (Patat et al. 1996; Parrent et al. 2012). Whether or not Fe II supersedes Si II at any given epoch, the velocities inferred from their respective absorption minima are still consistent with forming near the same projected velocity space to within 1500 km s^{-1} (see top of Figure 2).

However, the difference between a measured Si II and Fe II Doppler velocity for SN Ibc is not usually within typical errors of $500 - 1500 \text{ km s}^{-1}$ (Clocchiatti & Wheeler 1997; Elmhamdi et al. 2007; Milisavljevic et al. 2015). If the difference in Si II and Fe II Doppler velocities happens to be less for SN Ibc, this does not then favor Si II as a well-determined identification in SN Ibc spectra, particularly when one author’s emission feature is another author’s absorption signature (see McLaughlin 1961). In other words, a Si II line velocity is not more indicative of photospheric velocities than lines of Fe II if the feature attributed to Si II is not Si II.

Meanwhile, there is the classically defined SN Ic 1987M where an identification of the 6250 \AA absorption feature as weak Si II $\lambda 6355$ is difficult to rule out alongside robust detections of C II $\lambda\lambda 6580, 7234$ (Wheeler et al. 1995). However, similar to $\text{H}\alpha$ in the spectra of SN Ibc, an identification of “weak Si II” is based on a single doublet, $\lambda 6355$, where detections of other doublets, e.g. $\lambda 5972$, are difficult to rule in, if ever reported (cf. Figure 3).

At the same time, Doppler velocities of Si II and Fe II also conflict when $6000 - 6300 \text{ \AA}$ features in the spectra of broad-lined SN Ic (BL-Ic) and type I/R superluminous supernovae (SLSN) are interpreted to be either Si II or a Si II-based prescription of lines (Mazzali et al. 2000; Inserra et al. 2013; Lyman et al. 2014). Specifically, Si II-based model spectra are consistently too blue compared to the data (Baron et al. 1999; Branch et al. 2006). By contrast, observations of would-be conspicuous signatures of hydrogen in the spectra of BL-Ic and SLSN-I indicate that the emission component of $\text{H}\alpha$ undergoes a significant blue-ward shift relative to the rest wavelength of 6563 \AA (see Figure 1), which is an effect known to arise from steep density-gradients in the outermost ejecta of SN II in general (Baron et al. 1995; Anderson et al. 2014).

Thus, the discordant interpretation of Si II $\lambda 6355$ over $\text{H}\alpha$ is an important matter to address since it leads to inaccurate estimates of abundances, while also leaving the extent of hydrogen-depleted envelopes or clumps unexplored. In §2.1 we review the ability of various explosion models to reproduce Si II 6150 \AA features in the spectra of SN Ia. In §2.2 we report on the ability of various synthesizers to reproduce observations of SN Ibc assuming either a Si II $\lambda 6355$ feature or Si II-based prescription has been identified. We also discuss the status of $\text{H}\alpha$ as a likely identified signature and suitable alternative to Si II $\lambda 6355$ for a majority of SN Ibc. In §2.3 and §2.4 we address the same issues for the myriad of faint SN I and BL-Ic, SLSN, respectively. In §3 we summarize our findings and briefly discuss implications for progenitors.

2. ON THE $6000 - 6500 \text{ \AA}$ REGIONS OF TYPE I SPECTRA

Type I and Type II Supernovae

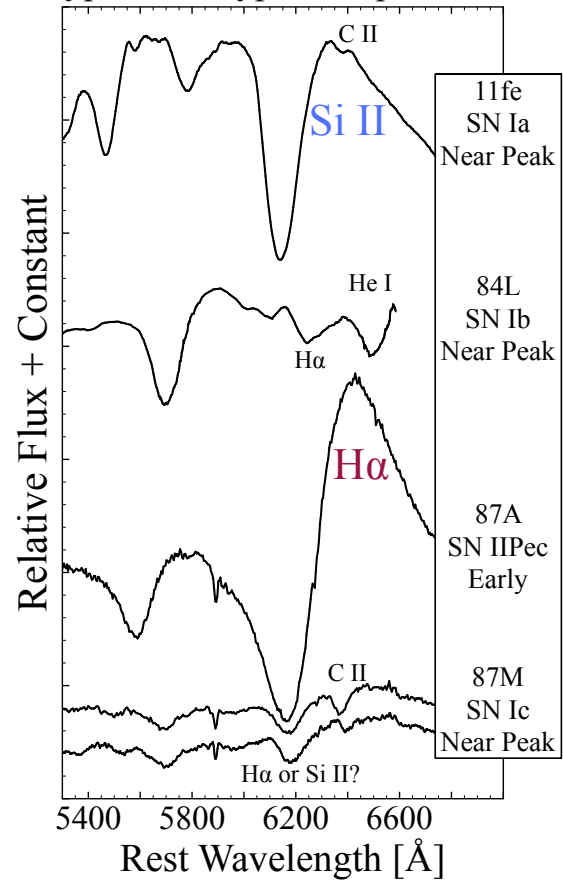


Figure 1. Zooming in on Fig. 1 of Filippenko (1997) after a relabeling of features. Spectrum references: SN 1987A soon after the explosion on UT February 24, 1987 (Pun et al. 1995); the spectra for SN 1984L (Filippenko 1997), SN 1987M (Filippenko et al. 1990; Jeffery et al. 1991), and SN 2011fe (Pereira et al. 2013) are near peak brightness.

In the sections below we review the latest model comparisons to type I spectra between 6000 and 6500 \AA . In Table 3 we summarize our findings in terms of the likelihood that hydrogen has been detected for various type I and type II events.

2.1. *Si II $\lambda 6355$ profiles in SN Ia spectra*

Plotted in Figure 4 are model comparisons for various spectrum synthesizers and observed SN Ia subtypes at wavelengths spanning $5200 - 7000 \text{ \AA}$. All models, ranging from semi-empirical to full non-LTE radiation transport solvers are capable of providing satisfactory fits to the feature centered about 6150 \AA .

In most cases, a non-standard distribution of Si II, or two distinct components of photospheric and detached Si II $\lambda 6355$, is evident for most SN Ia early on and blended near maximum light. In spite of this, the model spectra in Figure 4 are well-matched. Specifically, all absorption and emission components are well-centered with the data. Moreover, the curvature of the profile wings are well-matched as well; precise and accurate predictions are achieved for the red and blue wings, which are both sensitive to mean expansion velocities and the radial decline in density.

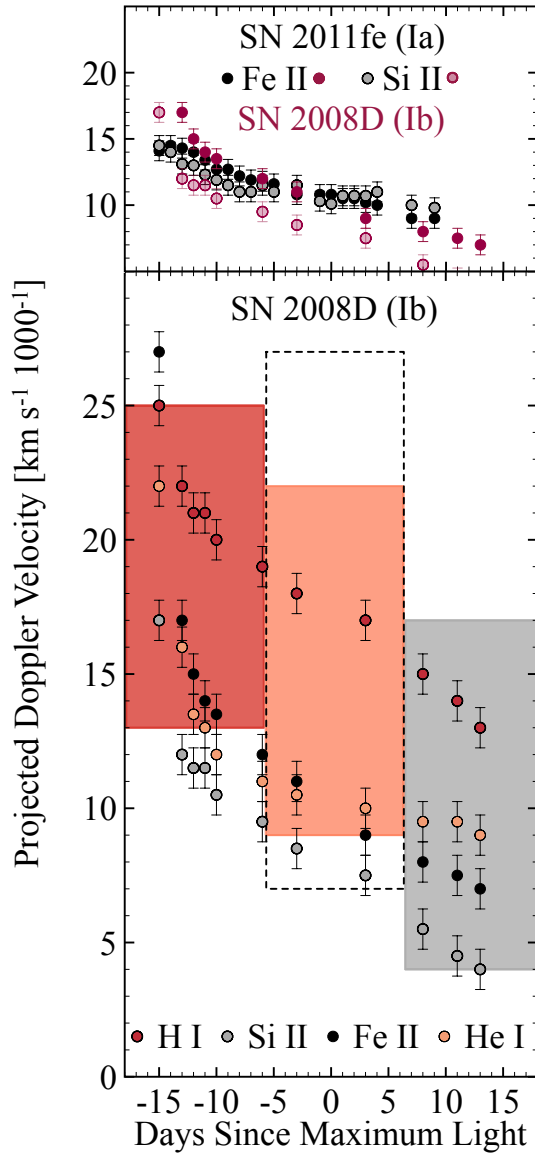


Figure 2. Here we detail for the first time estimated projected Doppler velocities of SN Ib 2008D from its absorption minima (Soderberg et al. 2008a; Modjaz et al. 2009). Estimates for He I $\lambda 5876$ and Na I are provided (in peach) to contrast different compositional interpretations. H I is shown in red, while an interpretation of Si II for the same feature is shown in grey. Vertical error bars shown for Si II and Fe II represent a conservative error of ± 750 km s $^{-1}$. The tops and bottoms of the shaded bounding boxes represent the same pre- and post-maximum light phases for each ion; i.e. velocities of Fe II are consistent with being well above regions of Si II in SN Ib 2008D. Shown above is SN Ia 2011fe to contrast the overlap of Si II and Fe II with that of SN Ib 2008D.

One reason a model SN Ia might not match perfectly near the emission component of the Si II is when the model does not center C II $\lambda 6580$ at approximately the same projected Doppler velocities as Si II during the first month post-explosion (Taubenberger et al. 2011; Pereira et al. 2013). Other lines that impact this region for SN Ia include S II $\lambda 6305$ and lines of Fe II near maximum light and thereafter. Despite these additional biases on direct measures of Si II Doppler velocities, the identification of Si II $\lambda 6355$ as a dominant line in the spectra of SN Ia is robust and a relatively flawless match for all spectrum

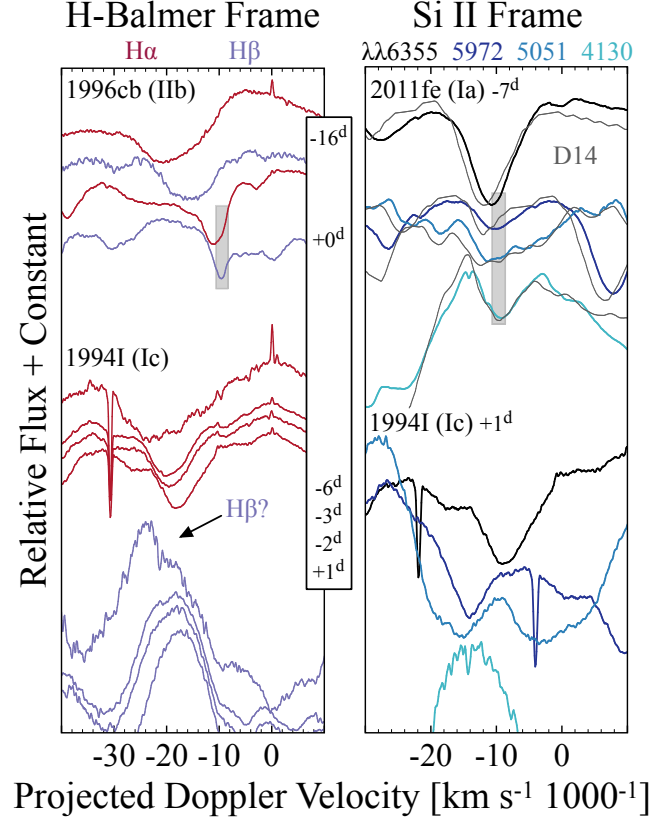


Figure 3. Plotted above are project Doppler velocities in the frame of the most likely detectable H-Balmer lines (left) and Si II lines (right). The grey bands are meant to indicate the overlap between common signatures of a given ion. Spectrum references: SN 1994I (Modjaz et al. 2014); SN 1996cb (Matheson et al. 2001); SN 2011fe (Pereira et al. 2013). Model references: (D14) PDDEL4, day -6.6 for SN 2011fe by Dessart et al. (2014).

synthesizers, as well as for a variety of normal and peculiar events.

To further appreciate the robustness of 6150 Å features in SN Ia spectra as having been identified as Si II $\lambda 6355$, consider that an intrinsic difference of 500, 1000, and 2000 km s $^{-1}$ mean expansion velocities would be reflected by an underlying line-shift of $\sim 10, 20$, and 40 Å, respectively. That is, significant differences of 2000 km s $^{-1}$ give rise to 40 Å blue-shifts that are of similar order to redshifts seen for 6150 Å features during the first month of free expansion. Despite these differences, model spectra for SN Ia fit a suite of observations fairly well (Figure 4).

When confronted by events like SN Ia 2012fr (Childress et al. 2013; Maund et al. 2013), where the conspicuousness of a high velocity (HV) signature of Si II $\lambda 6355$ is sensitive to the cadence of follow-up observations, approximate consistency with compound features near 6150 Å is relatively large for SN Ia. In other words, the relative location of HV Si II would not be well-constrained without the accompanying time-series spectra. This window of consistency is even greater for broad-lined SN Ic (BL-Ic) and SLSN.

2.2. H I and Si II as candidate identifications for SN Ibc

In contrast to all SN Ia, a confirming signature of Si II $\lambda 5972$ signature is not definitively detected for SN 1987M and most other SN Ibc (cf. Figure 3). A lack

of obvious Si II $\lambda 5972$ is to be expected since the stronger Si II $\lambda 6355$ would already be a weak signature compared to that for SN Ia, much less for the weaker Si II $\lambda 5972$. Thus the identification of Si II $\lambda 6355$ has only one point of constraint. Other ions like H I, O I, Na I, etc face the same obstacle during photospheric phases as well.

Plotted in Figures 5 and 6 is a collection of model comparisons to so-called “stripped-envelope” supernovae. To give favorable handicap to the interpretation of Si II, we have chosen epochs near maximum light and thereafter, where Si II $\lambda 6355$ is reported to either dominate or serve to shape features in the vicinity of 6250 Å. All model comparisons have been scaled to preserve presentation in the original works. For SN Ic 2007gr and Ib 2008D, we have digitized the full fit and the normalized Si II profile provided in Fig. 13 of Dessart et al. (2012); our conclusions below are the same for the single-ion fit of Si II as they are for the full fit in F_λ .

Cross-comparisons between a model geared for a particular supernova and observations from a different event is somewhat of a delicate matter. However, for cases where a detailed model is not available, e.g. SN Ib 1990I and Ib 2009jf, we use the normalized Si II profile produced for SN Ic 2007gr and Ib 2008D to approximate where nominal Si II would show up in these other hydrogen-poor events. These model Si II $\lambda 6355$ profiles, labeled as D12 07gr and D12 08D, correspond to mean projected Doppler velocities of 6000 and 9000 km s⁻¹, respectively. Thus our conclusions are strictly limited to the relative location of a given profile as a function of wavelength; i.e., we can say little to nothing precise about relative abundances.

2.2.1. SN Ib 1984L and SN Ic 1987M

Comparison of the early H α feature of SN IIPec 1987A to the 6170 Å feature of SN Ic 1987M in Figure 1 reveals an interpretation of H α is arguably more convincing than weak and putatively low velocity Si II $\lambda 6355$. Furthermore, in the spectrum of SN Ib 1984L, a He I $\lambda 5876$ feature centered about ~ 5750 Å implies line formation is approximately located at a mean projected Doppler velocity of 9000 ± 500 km s⁻¹. Looking red-ward in Figure 5 to the feature centered about 6250 Å, we see that both the blue model Si II profile corresponding to a projected Doppler velocity of 9000 km s⁻¹ (D12 08D), and the orange model Si II profile corresponding to a projected Doppler velocity of 6000 km s⁻¹ (D12 07gr), do not reproduce the data. If we had chosen to plot a Si II profile at 8000 ± 500 km s⁻¹, then the mismatch near 6250 Å would be worse than for the orange model at 6000 km s⁻¹, thus ruling out identification of Si II in SN Ib 1984L.

That said, there does exist fair visual agreement between the 6170 Å feature in SN Ic 1987M and the 9000 km s⁻¹ Si II profile produced by Dessart et al. (2012) for SN Ib 2008D; in our Figure 6, comparison with a model profile of Si II is arguably convincing. However, SN 1987M is the only SN Ic where Si II and H α are equally plausible interpretations since the epoch of the only available early spectrum (\sim day +7) is not early enough to confirm tentative detections of weak helium lines (Jeffery et al. 1991). If the feature is in fact H α , this would make sense given that the wings of the observed

Si II in Type Ia Supernovae

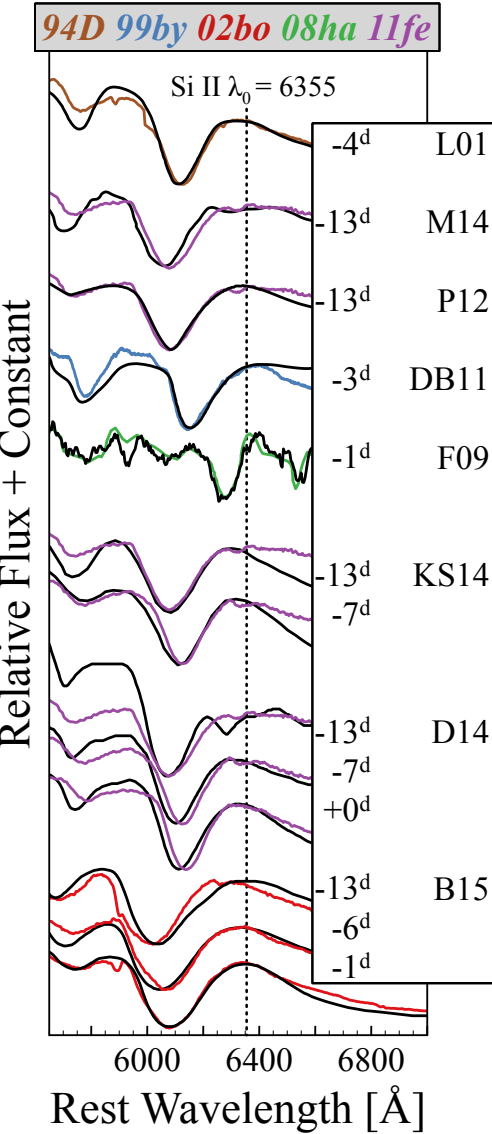


Figure 4. Model comparisons for a selection of SN Ia. Spectrum references: SN 1994D (brown), Patat et al. (1996); SN 1999by (blue), Garnavich et al. (2004); SN 2002bo (red), Benetti et al. (2004); SN 2008ha (green), Foley et al. (2009); SN 2011fe (purple), Parrent et al. (2012); Pereira et al. (2013); Mazzali et al. (2014). Model references: (L01) Lentz et al. (2001); (M14) Mazzali et al. (2014); (P12) Parrent et al. (2012); (DB11) Doull & Baron (2011); (F09) Foley et al. (2009); (KS14) Kerzendorf & Sim (2014); (D14) Dessart et al. (2014); (B15) Blondin et al. (2015).

feature are distinctly sharper than Si II-based models thus far.

The historically classified SN Ic 1987M appears to show signatures of C II $\lambda\lambda 6580, 7774$ as well (Wheeler et al. 1995), which is oddly similar to detections in SN Ia spectra. Narrow spectral features such as these indicate a limited span of projected Doppler velocities, perhaps due to an intervening hydrogen-depleted and oxygen-enriched envelope, which may be linked to the strength of the O I $\lambda 7774$ forming out ahead of C II and tentative regions of H I (cf. Matheson et al. 2001).

2.2.2. *SN Ib 1954A, 1999dn, 1999ex, 2005bf*

The search for signatures of hydrogen was first instigated by Branch (1972) who proposed the detection for SN Ib 1954A. As it turns out, this detection of faint H α is distinct compared to that for SN I Ib, where signatures of hydrogen are similar to SN II (Filippenko 1988). Later analyses of SN Ibc spectra by Wheeler et al. (1994) (and later Deng et al. 2000; Branch et al. 2002) favored the interpretation that 6250 Å features of normal SN Ibc are faint signatures of H α , thereby indicating the presence of a small amount of hydrogen-rich material out at higher than photospheric velocities.

PHOENIX model spectra of James & Baron (2010) have since given credence to these notions (some of which are derived from SYNOW analyses), showing that high velocity extensions of hydrogen-rich material for SN Ib 1999dn, with masses on the order of $M_H \lesssim 10^{-3} M_\odot$ assuming standard solar composition shells, provide a more suitable match and flexible alternative to ill-defined weak Si II features of SN Ib (see top of Figure 5). Supplemental data of SN 1999dn from Benetti et al. (2011) have further supported identification of H α in SN Ib spectra. The normal SN Ib 1999ex and the peculiar SN Ib 2005bf have provided strong evidence for conspicuous signatures of unburned hydrogen as well (Anupama et al. 2005; Follatelli et al. 2006; Parrent et al. 2007).

2.2.3. *SN Ib 1990I, 2008D, 2009jf*

For SN 1990I and 2009jf, two SN Ib where blue-shifts for the remaining He I features are greater than those of SN 2008D, the Dessart et al. (2012) model Si II profile is still too blue to confidently draw association between Si II $\lambda 6355$ and the feature near 6200 Å. Specifically, the Si II profile computed for SN 2008D by Dessart et al. (2012) is too blue overall and the blue-most wing is too shallow, regardless of artificial scaling factors (see Figure 5). By contrast, this symptom of “too blue” is not seen for SN Ia synthetic spectra made with the same CMFGEN for SN 2002bo and SN 2011fe (see Figure 4). Therefore, while Si II may be present in the ejecta of SN Ib, it is neither visually detected, nor is it significantly shaping 6250 Å feature.

2.2.4. *SN Ic 1994I*

As was seen for SN Ic 1987M above, the identity of features near 6170 – 6270 Å is a bit murkier for SN Ic than for SN Ib due to relatively weaker line strengths. Still, the same discrepancy found above for ~ 6200 Å spectral features of SN Ib is also recovered among those Si II-based models intended for SN Ic like 1994I and 2007gr. In fact for SN 1994I, a so-called “standard SN Ic”, two opposing interpretations prevail in the literature for the same mismatched Si II-based model.

Sauer et al. (2006) predict the feature centered about 6200 Å in the photospheric phase spectra of SN Ic 1994I is primarily a product of C II, Ne I, and Si II, with mostly Si II present near maximum light. Based on their series of model spectra, including the fit near maximum light shown in Figure 6, Sauer et al. (2006) claim a satisfactory match has been made.

Meanwhile, Branch et al. (2006) use SYNOW to show that a satisfactory solution is obtained for SN Ic 1994I

Type Ib-like Supernovae Model Si II vs. H α

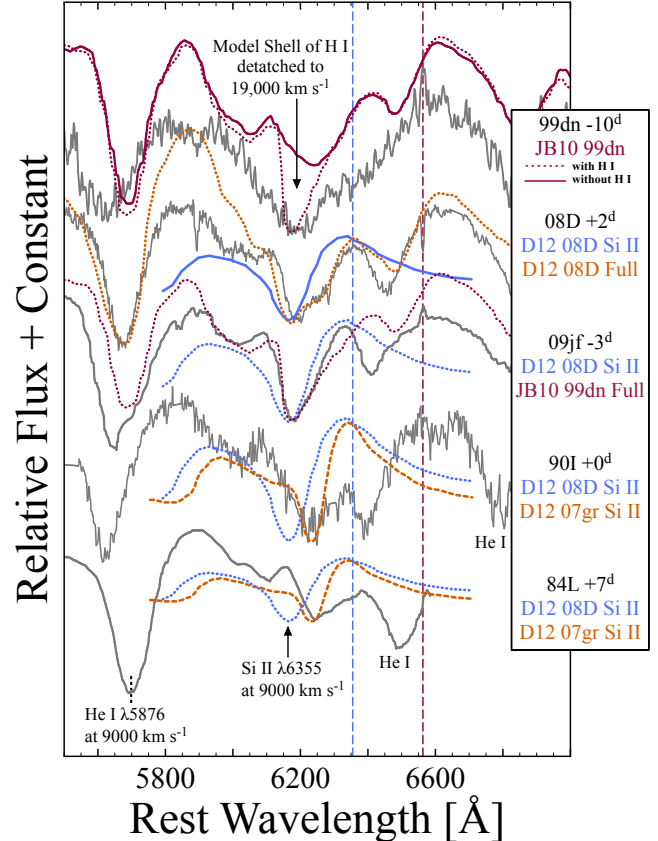


Figure 5. Model comparisons to a grab-bag of SN Ib-likes. Some observed features are labeled by those atomic species thought to dominate particular features and are not meant to imply the same for model spectra, e.g., S06 and B06 which both produce a strong signature of Si II $\lambda 6355$. Vertical-dashed lines denote the rest wavelength of Si II $\lambda 6355$ (blue) and H I $\lambda 6563$ (red). Spectrum references: SN 1984L (Filippenko 1997); SN 1990I (Elmhamdi et al. 2004); SN 1999dn (Deng et al. 2000); SN 2008D (Soderberg et al. 2008b); SN 2009jf (Valenti et al. 2011). Model references: (JB10) PHOENIX calculation of James & Baron (2010) with and without hydrogen are shown as the dashed and solid line, respectively; D12 07gr, D12 08D from Dessart et al. (2012) correspond to mean projected Doppler velocities of ~ 6000 and 9000 km s $^{-1}$, respectively.

near maximum light when He I, O I, Ca II, Ti II, and Fe II are assumed to form within similar strata of ejecta. When Branch et al. (2006) incorporate Si II into the SYNOW fit, the predicted offset of the feature dominated by Si II is nearly identical to that found by Sauer et al. (2006) (see Figure 6). This shows that spectrum synthesizers like SYNOW/SYNNAPPS and ARTIS/TARDIS are all equally capable of determining when Si II works for SN Ia, while mismatched model spectra can also reveal when a prescription of Si II will not work for most SN Ibc on account of being too blue (Baron et al. 1999), or not well-centered (Branch et al. 2007).

The case for hydrogen in SN Ic 1994I was reconsidered by Wheeler et al. (1994), while Clocchiatti et al. (1996) claimed detections of weak lines of He I as well. Both interpretations were later favored by Parrent et al. (2007) who used SYNOW to show that both PV and HV H I $\lambda 6563$ offer better alternatives to Si II-based models of Sauer

et al. (2006) and Branch et al. (2006).

Spectroscopic mismatch with a Si II-based prescription for SN Ibc is often interpreted to be either a reflection of a shallow density profile for the model, or a prescription that is out of sync with the time-series observations. Consequently, this has given rise to an interpretation that is counter to model comparisons shown in Figures 4, 5 and 6. For example, Hachinger et al. (2012) use the mismatched Si II-based model of Iwamoto et al. (1994) to argue that Si II is a viable option for the 6250 Å feature in SN 1994I and that this Si II feature is contaminated by other species including H α . In other words, despite offering to remedy the mismatch of model spectra with increased contribution from H α , the hydrogen/helium-enriched C+O models of Hachinger et al. (2012) remain dominated by ill-defined Si II λ 6355 and do not reflect the data of SN Ic 1994I.

When compared to the previous attempts, e.g. of Baron et al. (1999), Sauer et al. (2006), and Branch et al. (2006), all Si II-based models of Hachinger et al. (2012) also exhibit blended P Cygni profiles near 6150 Å that are “too blue” to draw association to 6250 Å features in the spectra of SN Ibc. It then follows that, instead of a Si II-identified feature contaminated by H α , at most Si II can contribute a small amount to the blue-most side of the 6250 Å feature, whereas the 6250 Å absorption minima in most SN Ibc spectra are dominated by hydrogen.

For most Si II-based model spectra, the inability of Si II to match observations of SN Ibc is often justified in that this Si II-based region is shaped by a time-dependent, multi-component prescription of species including He I, C II, Ne I, and Fe II (Hachinger et al. 2012). It is reasonable to expect a multi-component prescription throughout the spectrum of SN Ibc. However, it is unreasonable to suspect a correct interpretation for over-prescribed C II, Ne I, and Si II when the model used to support this prescription is incapable of producing the complex evolution of the data (Baron et al. 1999; Branch et al. 2006).

2.2.5. SN Ic 2007gr and SN Ic 1990B

Moving on to the September 10 spectrum of SN Ic 2007gr, Dessart et al. (2012) predict the feature centered about 6350 Å is a composite of Si II on the blue wing forming at ~ 6000 km s $^{-1}$ and Fe II near the minimum and reward (see also Valenti et al. 2008). For the full fit, the model spectrum in this region is promising, however the projected Doppler velocities of the model are too high overall.

Validation of the synthetic spectrum for SN 2007gr could benefit, e.g., by a modest reduction of the kinetic energy released. (This was done by Branch et al. 2002 who used SYNOW to interpret and measure Fe II lines in SN Ic 1990B.) However, the Si II would still remain too blue to confidently associate Si II with the absorption minimum of the 6350 Å feature, as is done in practice, otherwise the model spectrum would fail to match absorption minima elsewhere. Meanwhile, the model produces Si II λ 5972 feature not observed for SN Ic 2007gr (see bottom of Figure 6).

Also, there is less of a “Si II” notch on the blue wing of the larger 6350 Å feature to constrain the model when the spectrum is corrected for telluric features (Modjaz

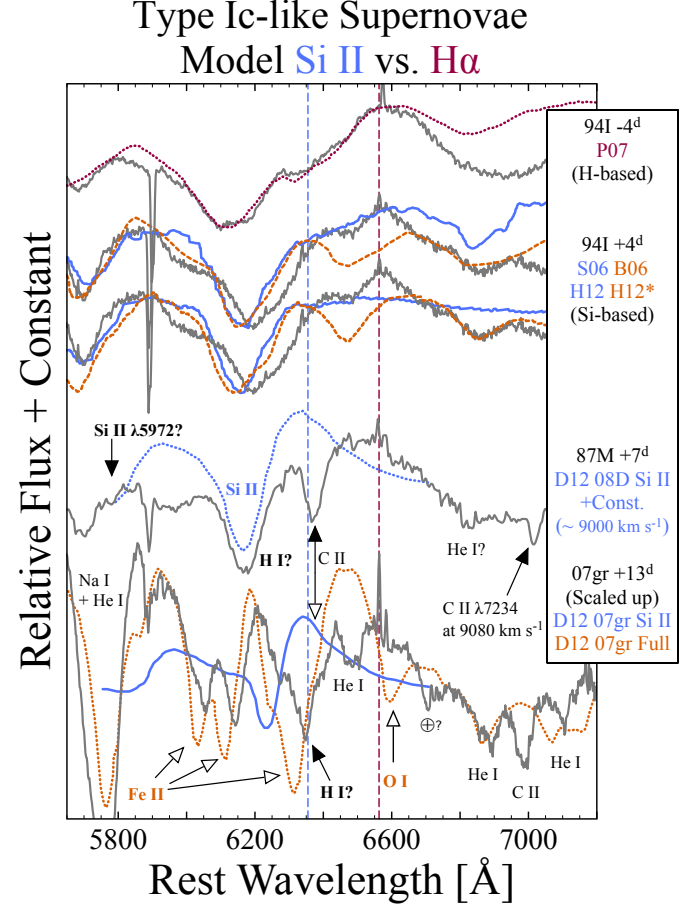


Figure 6. Like Figure 5, but model comparisons to a grab-bag of SN Ic-likes. Some observed features are labeled by those atomic species thought to dominate particular features and are not meant to imply the same for model spectra. Vertical-dashed lines denote the rest wavelength of Si II λ 6355 (blue) and H I λ 6563 (red). Spectrum references: SN 1987M (Jeffery et al. 1991); SN 1994I (Modjaz et al. 2014); SN 2007gr, telluric corrected (Modjaz et al. 2014). Model references: (P07) SYNOW calculation of Parrent et al. (2007) with hydrogen for SN Ic 1994I (JB10) PHOENIX calculation of James & Baron (2010) with hydrogen for SN Ic 1999dn; D12 07gr, D12 08D from Dessart et al. (2012) correspond to mean projected Doppler velocities of ~ 6000 and 9000 km s $^{-1}$, respectively; (S06) Sauer et al. (2006); (B06) Branch et al. (2006); H12 models are from Hachinger et al. (2012). The blue model, H12, is the base SN Ic 94I mod. 16 days after explosion in the top of their Fig. 11 in green. The orange model, H12*, corresponds to the hydrogen-enriched SN Ib in the top of their Fig. 11 in red. Like S06 and B06, both Si II-based H12 models fail to match the feature at 6250 Å in SN Ic 1994I.

et al. 2014). Subsequently, we find the detection of Si II in SN 2007gr to be either unlikely and therefore not representative of “Si II features” of SN Ibc in general, or contribution from Si II λ 6355 is minimal and blue-ward of 6250 Å like it is for SN II and IIb (Baron et al. 1995; Dessart & Hillier 2006).

2.3. On the Zoo of Peculiar SN I

In Figure 7, we have plotted a zoo of peculiar SN I where the primary origin of a 6250 Å feature is questionable. For comparison to the evolution of blended Si II λ 6355 profiles in SN Ia, the day -15, maximum light, and day +15 spectra of SN Ia 2011fe are shown. We also plot the SN IIb 1993J and SN IIP 2005cs

post-maximum light spectra as references for projected Doppler velocities among these hydrogen-positive events.

2.3.1. SN 2002bj and 2006jc

Luminous SN Ibn like 2006jc produce conspicuous narrow emission lines of He I and Si II, whereas other SN Ibn-like events, e.g. SN 2002bj, reveal curious P Cygni signatures in addition to relatively broad C II emission (Poznanski et al. 2010). It is questionable, however, as to whether the spectra of SN Ibn and SN 2002bj exhibit blue-shifted absorption due to Si II $\lambda 6355$. By contrast, and from an apparent lack of narrow emission near 6563 Å, the presence of significant quantities of hydrogen in the helium-rich zone of narrow emission is unlikely; the emission feature is likely constructed from [N II] emission lines that flank 6563 Å (Pastorello et al. 2006; Anupama et al. 2009).

2.3.2. PTF09dav

The peculiar PTF09dav was first classified as a SN Ia due to overall similarities to faint SN Ia, but was later re-classified as a faint Ca-rich transient (Sullivan et al. 2011; Kasliwal et al. 2012). Here the identification of low velocity Si II is unclear albeit reasonable considering the spectrum is littered with narrow spectral features elsewhere. However, Kasliwal et al. (2012) identify narrow and weak hydrogen emission during nebular phases, which would make the case for an early detection of hydrogen more likely.

2.3.3. SN 2012hn

As for the peculiar and faint SN 2012hn, its multi-component 6325 Å feature is similar to SN 2007gr in some ways (Valenti et al. 2014). Namely, and barring possible contamination from sharp telluric features, if Si II $\lambda 6355$ is an active line in SN 2012hn, then it is strictly limited to shaping the feature blue-ward of 6250 Å. An added prescription of Fe II would be able to explain the minimum at 6325 Å if it were not for a lack of Fe II at 6110 Å. There is also room for the strongest He I lines to be weakly present. Therefore, we favor a hydrogen-positive interpretation over Si II for SN 2012hn as well.

2.3.4. SN 2005ek and 2010X

For the fast-evolving and faint SN 2005ek and 2010X, weak contamination from H I $\lambda 6563$ and He I $\lambda 5876/\lambda 6678$ is fairly ambiguous against plausible detections of Si II $\lambda 6355$ and Na I $\lambda 5889/C$ II $\lambda 6580$, respectively. That said, mean projected Doppler velocities between weak He I, Na I, and Si II are not too dissimilar to rule out Si II for SN 2005ek and 2010X (Drout et al. 2013).

2.4. H I and Si II as candidate identifications for Broad-lined SN Ic and Super-luminous Supernovae

The same distinctions used for classical types I and II are used for super-luminous supernovae as well; SLSN-II denotes the presence of conspicuous hydrogen while SLSN-I like SN 2007bi and LSQ12dlf are said to be without a hydrogen feature, or even so far as “hydrogen-free”. However, here too this definition can be misleading, as we discuss below. It is also unclear if the class of SLSN

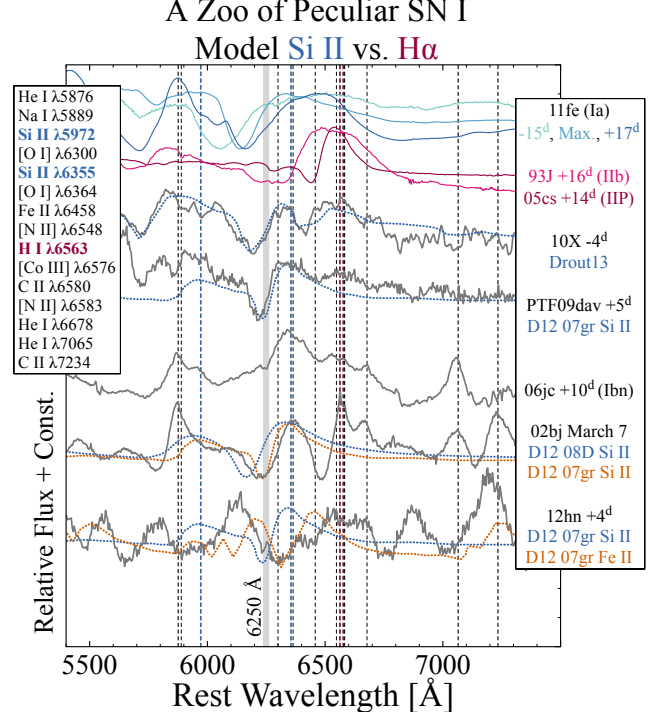


Figure 7. Comparisons of a zoo of type I events. From left to right, vertical dashed lines indicate rest wavelengths for Si II $\lambda 6355$, Fe II $\lambda 6458$, and [Co III] $\lambda 6576$. (These lines are for reference and do not indicate detections.) Spectrum references: SN 1993J (Barbon et al. 1995); SN 2002bj (Poznanski et al. 2010); SN 2005cs (Pastorello et al. 2006); SN 2006jc (Anupama et al. 2009); PTF09dav (Sullivan et al. 2011); SN 2010X (Kasliwal et al. 2010); SN 2011fe (Pereira et al. 2013); SN 2012hn (Valenti et al. 2014). Model references: Drout13 is the full Si II-based model including He I, and where C II cannot be ruled out (Drout et al. 2013); D12 07gr, D12 08D from Dessart et al. (2012) correspond to mean projected Doppler velocities of ~ 6000 and 9000 km s $^{-1}$, respectively.

powered by radioactive decay through pair instability (type R) has been observed, or if these and other BL-Ic fall under another category of hydrogen-poor core-collapse supernova (Gal-Yam et al. 2009; Moriya et al. 2010; Yoshida & Umeda 2011; Dessart et al. 2013).

It is true that SLSN-II show signatures of hydrogen, however the hydrogen feature is so far like that of a SN IIn, i.e. a narrow emission signature of hydrogen, e.g., SN 2006gy (Smith et al. 2007) and 2008am (Chatzopoulos et al. 2011). For SLSN-I, a feature in the vicinity of 6000 – 6300 Å is either truly absent or faint, or a large P-Cygni feature exists that is often attributed, again, to Si II-based prescriptions.

However, close inspection of comparisons in Figure 8 between Si II-based models reveal an insufficient match for SLSN. In fact, a familiar mismatch of “too blue” is observed on multiple occasions for these fully-stripped C+O models from Iwamoto et al. (1994), and either without any improvement in subsequent adaptations to BL-Ic and SLSN, or with the same conclusion of a model with a relatively shallower density profile when compared to data (see model references in Figure 8 below).

2.4.1. BL-Ic 1997ef, 1998bw, 2002ap, 2003dh, 2003lw

For BL-Ic 1998bw, the model fit is too blue. Specifically, the rest-wavelength emission component produced for SN 1998bw is nearly 100 Å too blue to match obser-

vations without considerable absorption via *ad hoc* prescriptions of C II and Ne I. However, if the model were improved near 6200 Å with C II and Ne I, these ions would be at odds with the data at other wavelengths (Elmhamdi et al. 2006, 2007).

As for BL-Ic 2002ap (Foley et al. 2003), the 9000 km s⁻¹ Si II profile from Dessart et al. (2012) reveals similar problems of “too blue” without an *ad hoc* prescription of adjacent species that are not strongly detected elsewhere. In particular, the discrepancy in the curvature produced by the Si II model profile and what is observed is a tell-tale sign that Si II λ 6355 cannot be associated with the 6250 Å feature in BL-Ic 1998bw and 2002ap (cf. LSQ12dlf in Figure 8).

From Figure 8, the model fit for BL-Ic 1997ef from Mazzali et al. (2000) looks promising near the absorption minimum. However, as a whole, it seems the CO21 (Iwamoto et al. 1994) and CO138H (Iwamoto et al. 1998) models associated with the assortment of mismatched synthetic spectra are better suited for other supernovae yet to be observed. Moreover, the emission feature peaking at \sim 6355 Å is more reminiscent of the emission region near 6300 Å in SN Ibc like 2006jc (cf. Figure 7).

Similar conclusions apply to so-called “Hypernovae”, such as SN 2003hd (Deng et al. 2005) and 2003lw (Mazzali et al. 2006). For SN 2003dh, the Si II-based model spectrum provided conflicts with the observations throughout, including wavelength regions not shown in our Figure 8.

The Si II-based model spectrum of Mazzali et al. (2006) also falls short of rectifying a model spectrum that is “too blue” when compared to both SN 2003dh and 2003lw. We suspect any proposed solution of Si II + H I, and in similar respects to the results of Hachinger et al. (2012) discussed above for SN Ibc, will ultimately be less convincing.

2.4.2. BL-Ic 2010ah

Comparison between the the March 7 spectrum of SN 2010ah (PTF10bzf) and the model spectrum of Mazzali et al. (2013) are shown at the bottom of Figure 8. For this BL-Ic, Mazzali et al. (2013) utilize rescaled CO138 models of Iwamoto et al. (1998) to interpret spectral signatures. Here again, we see the model does not provide adequate predictions.

However, unlike previous comparisons to BL-Ic and SLSN, this is the first time in Figure 8 that we see the Si II-based prescription under-shoot the observed 6050 Å feature. Regardless, there are two ideal routes, and therefore two interpretations, for addressing the discrepancy between the synthetic spectra and observations of SN 2010ah. One could argue that the model predicts velocities that are not as high as the observations, and that a simple scaling of kinetic energies, or a shallower ejecta density profile, would address the mismatch, thereby shifting the model spectrum blue-ward for a satisfactory match. This is marginally true within the span of wavelengths plotted in Figure 8. However, such a correction for features near 6000 – 6300 Å would create additional mismatch already seen for Ca II and Fe II features at other wavelengths (shown in Fig 6. of Mazzali et al. 2013). Furthermore, the blue wing of the 6150 Å feature in the model conflicts with the observations, and

BL-Ic, GRB, SLSN-I/R Model Si II vs. H α

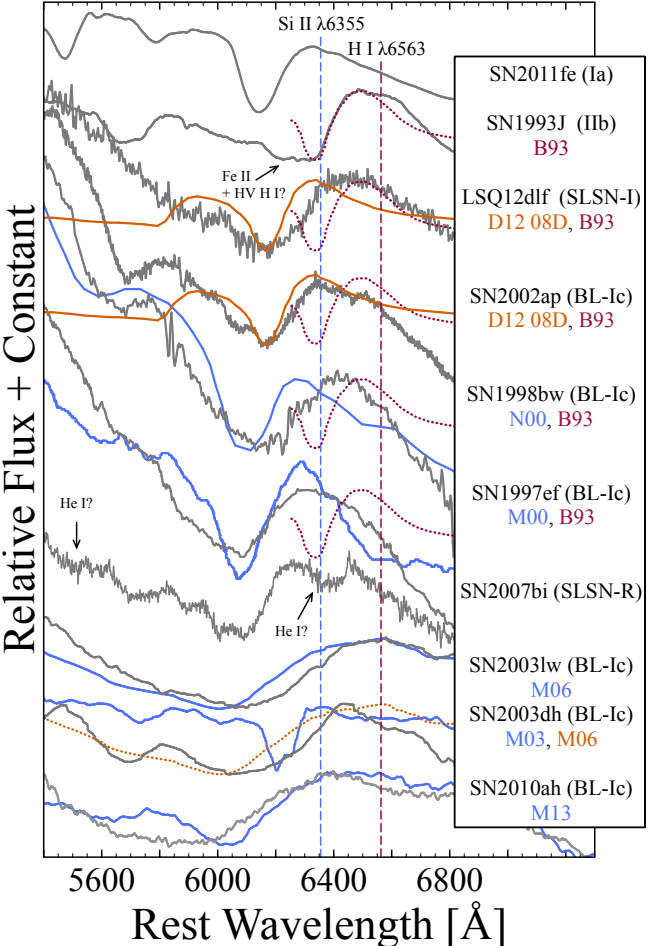


Figure 8. Model comparisons to a grab-bag of BL-Ic, SLSN, SN 1993J, and SN 2011fe. Spectrum references: SN 1993J (Barbon et al. 1995); SN 1997ef (Modjaz et al. 2014); SN 1998bw (Patat et al. 2001); SN 2002ap (Modjaz et al. 2014); SN 2003dh (Deng et al. 2005); SN 2003lw (Mazzali et al. 2006); SN 2007bi (Gal-Yam et al. 2009); SN 2010ah (Corsi et al. 2011); SN 2011fe (Pereira et al. 2013); LSQ12dlf (Nicholl et al. 2015). Model references: (B93) Baron et al. (1993); (D12 08D) Dessart et al. (2012); (N00) Iwamoto et al. (1998); (Nomoto et al. (2000); (M00) Mazzali et al. (2000); (M03) Mazzali et al. (2003); (M06) Mazzali et al. (2006); (M13) Mazzali et al. (2013).

similar to what is seen for SN 1997ef, 1998bw, 2002ap, 2003dh, and LSQ12dlf.

Alternatively, one could conclude the mismatch between the model spectrum does not correspond to the epoch needed for an appropriate comparison to SN 2010ah. In other words, had follow-up observations been issued, i.e. for more than the two spectra obtained for SN 2010ah, we suspect the CO138 model spectrum would appear “too blue” compared to the data near 6250 Å.

2.4.3. SLSN-I LSQ12dlf and SLSN-R 2007bi

For SN 2007bi, no model spectrum was provided by Gal-Yam et al. (2009). Based on the self-similarity between the spectrum of SN 2007bi and spectra in Figure 8, we see that the feature is not likely to be a product of Si II either. In fact, tentative detections of He I as in-

dicated in Figure 8 would favor identification of $\text{H}\alpha$ at 6200 Å.

Curiously, Nicholl et al. (2014, 2015) recently utilized SYNAPPS to identify Si II in the spectrum of another SLSN-I LSQ12dlf. (Comparison of the Si II profile for SN Ib 2008D to the spectrum of LSQ12dlf in Figure 8 provides the same conclusion as the original SYNAPPS fit.) Considering the observed feature slopes below the emission component of model Si II profile, the mismatch between the model and data is unavoidable, and the spectrum is too noisy to assess the underlying structure of this supposed compound-feature. Consequently, the interpretation of Si II as the 6250 Å feature in LSQ12dlf is clearly inconsistent with the data from red-most side of the emission component, through the absorption trough, and near the blue-most wing. Therefore, the SYNAPPS fit to LSQ12dlf shows that Si II-based prescriptions are not the most appropriate option for BL-Ic and SLSN-I/R.

2.4.4. $\text{H}\alpha$ $\lambda 6563$ as a candidate identification for Broad-lined SN Ic and Super-luminous Supernovae

Relative to $\text{H}\alpha$ in SN II spectra, SN IIb show weaker signatures of hydrogen alongside conspicuous helium lines (Filippenko 1988). Also, the $\text{H}\alpha$ profile for SN IIb is typically broader than that for SN II. Part of the reason, it turns out, is because the mass of the remaining hydrogen is greater for SN II than SN IIb; unburned hydrogen in the atmosphere of SN IIb 1993J is $M_H \lesssim 0.2 M_\odot$, and likely down from $M_H \sim 0.6 M_\odot$. Subsequently, the weakness of $\text{H}\alpha$ in SN IIb spectra enables adjacent blending from species like Si II, Fe II, and possibly higher velocity H I to artificially broaden the absorption component of the underlying $\text{H}\alpha$ P Cygni profile. Similar to SN IIP, the associated emission of $\text{H}\alpha$ found in SN IIb is observed to be shifted blue-ward from center for SN IIb as well (as much as 75 Å) (Baron et al. 1995; Milisavljevic et al. 2015).

Considering the self-similarity of all BL-Ic and select SLSN-I/R plotted in Figure 8, we find it more likely that a majority of the data reveal conspicuous signatures of $\text{H}\alpha$, rather than interpretations of Si II favored by consistently mismatched model spectra. One apparent obstacle for an interpretation of $\text{H}\alpha$ is that the classical defined rest-wavelength P Cygni emission component of the observed feature is not centered about a rest-wavelength of 6563 Å. By comparison, emission components of Si II $\lambda 6355$ for SN 2011fe would appear closer to 6355 Å if the lingering signature of C II $\lambda 6580$ was absent (see top of Figure 8).

One solution that would still favor the interpretation of hydrogen for BL-Ic and select SLSN-I/R would be if the emission component of $\text{H}\alpha$ is blue-shifted along with the corresponding absorption minimum. Blue-shifted emission components are common for $\text{H}\alpha$ in SN IIb like 1993J where the corresponding absorption feature is also carved out by Fe II (Baron et al. 1993) and possibly H I detached at higher velocities like that proposed for the transitional SN IIb/Ib 2011ei (Milisavljevic et al. 2013). For SN II, Anderson et al. (2014) have shown the blue-shifted emission of $\text{H}\alpha$ is sensitive to the ejecta density profile, particularly when the radial falloff is steep.

In other words, a better handling of the radiation transport—better than 1-dimensional photospheres—may

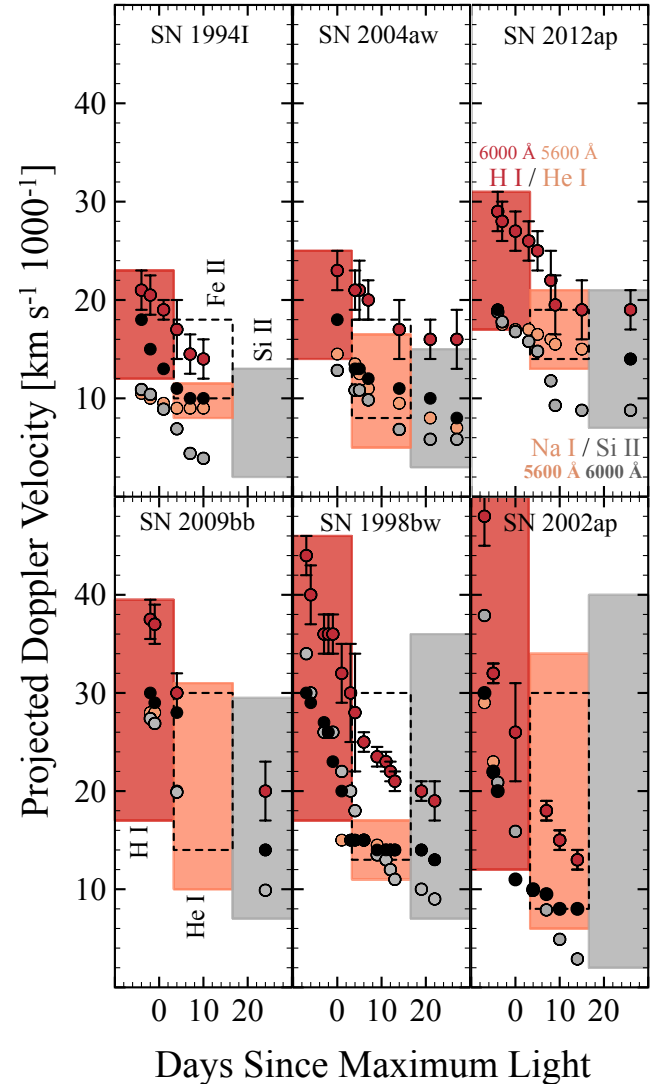


Figure 9. Here we detail projected Doppler velocities as shown through 6000 Å features in SLSN and BL-Ic spectra, and assuming interpretations of Si II $\lambda 6355$ (grey) are corrected to $\text{H}\alpha$ (red). Estimates for He I $\lambda 5876$ and Na I are provided (in peach) to contrast different compositional interpretations. Projected Doppler velocities for Fe II were extracted from the highly broadened lines of Fe II using SYNAPPS; see Parrent (2014) for fitting methods. Vertical error bars shown for H I represent the width of the 6000 Å per day and signify that contributions from additional lines are unclear with the available data. The tops and bottoms of the shaded bounding boxes represent the same pre- and post-maximum light phases for each ion; velocities of Fe II are consistent with being well above regions of Si II for SN 1994I, 1998bw, 2002ap, 2004aw, 2009bb, and 2012ap.

uncover such a mechanism for confirming and estimating the amount of remaining hydrogen-rich material in BL-Ic and SLSN. This would serve to solidify the interpretation of hydrogen for BL-Ic and SLSN-I/R, but would not help the situation for Si II.

2.5. Measures of projected Doppler velocity

For the extreme case of mismatch between the model and data, e.g. SN Ib 1984L in Figure 5 and LSQ12dlf in Figure 8, Si II $\lambda 6355$ is ruled a misidentification because the observed absorption feature is surpassed by the model emission region of Si II $\lambda 6355$, thereby making it

fundamentally impossible for the observed feature to be associated with Si II $\lambda 6355$. Even under less extreme circumstances, it is this condition of discordant projected Doppler velocities inferred from absorption minima that dictates when Si II $\lambda 6355$ is not either a conspicuous feature or legitimately detected for the majority of normal and peculiar SN Ib, Ic, BL-Ic, and SLSN-I/R. Consequently, absorption minima near $6100 - 6300 \text{ \AA}$ cannot be utilized in concert with $\lambda_0 = 6355 \text{ \AA}$ to chart an evolution of projected Doppler velocities over time (e.g., as done in Ben-Ami et al. 2012; Walker et al. 2014; Lyman et al. 2014; Benetti et al. 2014; D'Elia et al. 2015).

If absorption signatures from, e.g., He I, Ca II, and Fe II indicate projected Doppler velocities $\gtrsim 5000 \text{ km s}^{-1}$ near maximum light, then features near 6250 \AA are unlikely to be formed by atoms of singly ionized silicon (cf. Figure 7). More generally, if projected Doppler velocities of “Si II features” in the spectra of SN Ibc indicate values that are $1000 - 2000 \text{ km s}^{-1}$ below velocities inferred from signatures of He I, Ca II, and Fe II, then the feature identified with Si II is very likely a faint signature of hydrogen (Branch et al. 2006; Elmhamdi et al. 2007).

The effect that opposing interpretations of Si II $\lambda 6355$ versus $\text{H}\alpha$ has on estimates of mean projected Doppler velocities is shown in Figures 2 and 9; assuming one line dominates, the error is on the order of $\delta v \sim 9000 \text{ km s}^{-1}$ between Si II $\lambda 6355$ and $\text{H}\alpha$. (This is staggering.) By stark contrast, errors associated with degenerate interpretations of He I $\lambda 5876$ or Na I $\lambda 5889$ (or both) are similar to natural uncertainties of line blending for a single line detected, $\delta v \sim 600 \text{ km s}^{-1}$.

An interpretation of hydrogen invokes a layer residing naturally above layers of He I for all BL-Ic. The latter interpretation makes more sense than needing to invoke either gross mixing in the outer layers or explain a fairly unlikely situation of opaque iron well-above weak signatures of a lone Si II $\lambda 6355$ line. However, so-called detachment velocities for hydrogen are either accurate from first principles, or direct measurements are again spoiled by effects of radiation transport in that the resultant blue-shifted P Cygni profile is not indicative of a classical projected Doppler velocity. That is to say, under the assumption of either localized line formation ($\Delta\lambda/\lambda_0$), or multiple resonance line scattering (SYNAPPS), ejecta velocities inferred from absorption minima may over-shoot the optimum position of these ostensibly found hydrogen-deficient regions of ejecta.

If faint $\text{H}\alpha$ in SN Ib, Ic, BL-Ic, and SLSN-I/R behaves similarly compared to SN II and IIb, then trace amounts of hydrogen would indicate high projected Doppler velocities in spite of being relatively closer to the photospheric line forming region. Such “corrections” would only further support present notions that an association between $6000 - 6300 \text{ \AA}$ features in BL-Ic SLSN-I/R spectra and $\text{H}\alpha$ is correct (cf. Figure 1).

3. SUMMARY AND CONCLUSIONS

In this work we looked at Si II-based model spectra and compared them with observations from several SN Iabc subclasses, including super-luminous supernovae of type I/R. Apart from natural uncertainties from line blending ($\delta v \sim 500 \text{ km s}^{-1}$), and regardless of the spectrum synthesizer used, all model spectra intended for

thermonuclear SN Ia are well-matched (Figure 4). However, while the evidence for Si II $\lambda 6355$ in SN Ia spectra is overwhelming, the same cannot be said for numerous SN Ib, Ic, BL-Ic, and SLSN-I/R.

More specifically, in §2.1 we found that a satisfactory match to Si II $\lambda 6355$ profiles in SN Ia spectra is defined by well-centered emission and absorption components, in addition to well-matched red and blue wings of the line profile. Whether or not the Si II feature is due to photospheric and high-velocity components, these criteria are met for all models in Figure 4 and throughout the literature. Because of this, it is relatively straightforward to monitor the evolution of all SN Ia spectral features in order to fix relative contributions for an 11-component metric (Parrent 2014).

In §2.2 and §2.4, we reviewed the literature of models of SN Ib, Ic, BL-Ic, and SLSN-I/R purporting either an identification of Si II $\lambda 6355$, or a Si II-based prescription, and determined that none of the associated synthetic spectra shown in Figures 5, 6, and 8 provide a convincing match in spite of various spectrum synthesizers used. Thus primary stars that lose all of their hydrogen, e.g. those most similar to the models of Iwamoto et al. (1994, 1998), are disfavored for the majority of SN Ibc. The models of Mazzali et al. (2000, 2003, 2006, 2013) are also disfavored for the majority of BL-Ic and SLSN-I/R given that the models attribute what is likely to be blue-shifted signatures of $\text{H}\alpha$ with a less convincing Si II $\lambda 6355$ identification.

In actuality, when some hydrogen and helium are returned to the bare C+O parent models of Iwamoto et al. (1994, 1998) (e.g., as was attempted by Hachinger et al. 2012), the helium lines are primarily improved, but the H I remains mismatched on account of too much Si II (cf. Figures 5 and 6). This underscores the importance of having accurate synthetic spectra and densely sampled time-series observations, where model light curves provide a secondary tier of validation for a given explosion model.

In §2.2 and §2.4 we also reviewed evidence supporting detections of $\text{H}\alpha$ for SN Ib, Ic, BL-Ic, and SLSN-I/R, and we found the presence of unburned hydrogen to be likely for all subcategories (summarized in Table 3). Some notable exceptions do exist, namely SN 1987M, 2002bj, 2005E, and PTF09dav and 10iuv, where a bona fide interpretation of Si II $\lambda 6355$ is unclear. However we consider the presence of Si II here to be unrepresentative of the norm, if detected at all.

In other words, the most likely solution for the faint signatures in type I spectra near 6250 \AA is not more H I superposed with a dominant Si II line, nor more C II, Ne I, and Fe II as prescribed by some Si II-based models. Rather, signatures of $\text{H}\alpha$ are very likely the conspicuous 6250 \AA absorption features in many SN Ib, Ic, BL-Ic, and SLSN spectra, where any contribution from Si II $\lambda 6355$ is restricted to the blue-most wing, if present at all. This implies a significant result, namely that progenitor material remains for all three type Iabc subclasses (Branch 1972; Jeffery et al. 1992; Wheeler et al. 1995).

On their own, detections of hydrogen in the spectra of SN I and II provide clues about the chemical make-up and mass-loss history for a given progenitor system. For SN II, signatures of $\text{H}\alpha$ represent the remains of a

Table 1
Detectable Hydrogen by Supernova Type

SN Type	Prototypes	Detectable Hydrogen		
		Yes	Likely	Unclear
Ia	94D, 05cf, 11fe, 14J			X
Ia-pec	91bg (CL), 91T (SS), 84A (BL)			X
I-pec	02cx, 02es, 05hk			X
	05ek, 10X			X
†SLSN-I	05ap			X
Ibn	00er, 06jc			X
I-pec	87M			X
	02bj			X
	05E, PTF09dav, PTF10iuv (10et)			X
	12hn			X
†SLSN-II	07bi, 11ke, LSQ12dlf			X
BL-Ic	97ef, 98bw, 02ap, 03dh, 03lw, 09bb, 12ap			X
Ic	90B, 07gr			X
Ib/c-like	94I			X
Ia-CSM	05jg, PTF11kx		X	
IIn	88Z, 98S		X	
Ib	90I, 99dn, 05bf, 08D		X	
IIb	Cas A, 93J, 96cb, 03bg, 08ax, 11dh		X	
IIpec	87A, 97D, 98A		X	
IIIP/L	69L, 92H, 99em, 99gi, 04dj, 04et, 05es, 06bp		X	
†SLSN-IIIn	06gy, 08am		X	
SN Imposters	09ip		X	

[†] Reclassified assuming the blue-shifted P Cygni profile between 6100 and 6300 Å is H α (not Si II), whereas the previous SLSN-II has been reassigned to SLSN-IIIn in an effort to distinguish the kind of hydrogen emission detected. See §2.4.

red supergiant's hydrogen-rich envelope, while in some cases, e.g., SN 1987A, the progenitor is a blue-supergiant and/or luminous blue variable star (Smartt 2009; Burrows 2013 for reviews). Meanwhile, a red supergiant progenitor is found for the SN IIb 1993J (Aldering et al. 1994; Cohen et al. 1995) and a yellow supergiant progenitor has been identified in pre-SN archival images for the SN IIb 2011dh (Van Dyk et al. 2011). Stripping of the primary is likely to occur with a close companion (van Dyk et al. 1996; Nomoto et al. 1996), and most notably by a hot B star in the case of SN IIb 1993J and 2011dh (Maund et al. 2004; Fox et al. 2014). The exact kind of primary and secondary stars that are available to the production line of SN IIb may vary by the time of explosion, perhaps for both normal and peculiar SN IIb.

For SN Ibc, which are often assumed to be without faint signatures of hydrogen and helium in their spectra, full details on the primary and/or secondary stars are not yet given. Assuming a single star channel for hydrogen-poor events, detections of trace amounts of hydrogen and helium in the ejecta imply that the progenitor will not resemble hydrogen/helium-depleted Wolf-Rayet spectral types (WC, WO), nor WNE stars that, apart from some exceptions, have lost the entirety of their hydrogen envelopes prior to the explosion.

Alternatively, the most likely binary systems to produce SN Ibc will involve primaries with $8 \lesssim M/M_{\odot} \lesssim 17$ that reach helium core masses of $\sim 3.5 M_{\odot}$ (Bersten et al. 2014; Smartt 2015). A star at solar metallicity that undergoes mass transfer during the phase of helium contraction will retain $M \lesssim 0.1 M_{\odot}$ on its surface (Yoon 2015). If the mass of this core is $3 \lesssim M_{He}/M_{\odot} \lesssim 4.4$, then early photospheric phase spectra of SN Ibc indicate $M_H \gtrsim 10^{-4} - 10^{-2} M_{\odot}$ can survive a stellar wind prior to the explosion, as well as explosive burning during the supernova event.

Faint signatures of hydrogen for SN Ibc may instead indicate the presence of a companion that has retained a

thin shell of hydrogen. In this scenario, detections of H α suggest the material is either a by-product of the companion's own mass-loss, or material initially transferred to the companion. Similarly, an O-star that has not lost the entirety of its hydrogen prior to the explosion could enable detections of a diffuse common envelope in some instances. James & Baron (2010) computed PHOENIX synthetic spectra to show that the material needed in the atmosphere of SN Ib 1999dn to reproduce the 6250 Å feature ($M_H \lesssim 10^{-3} M_{\odot}$ assuming standard solar composition shells) is less than that inferred for SN IIb 1993J by Baron et al. (1995), and does not conflict with the swept-up $5 \times 10^{-2} M_{\odot}$ estimated from model comparisons to late-nebular spectra of SN IIb (Jerkstrand et al. 2015).

Thus, depending on the sample of hydrogen-poor supernovae used, correlations may exist between properties of the light curves and the extent and/or relative location of semi-detached regions of hydrogen. If divisions of hydrogen-poor shells or clumps are truly detached from the bulk of the ejecta below, and even mildly so, this would indicate characteristics of faint H α features are sensitive to properties of the binary. Given a suite of improved model spectra, faint signatures of H α in the ejecta of hydrogen-poor supernovae of type I could be used to probe any connections between mass loss rates and the extent of hydrogen near the surface of the progenitor star or binary product.

This work was made possible by contributions to the SuSupect (Richardson et al. 2001) and WISEREP databases (Yaron & Gal-Yam 2012), as well as David Bishop's Latest Supernovae page (Gal-Yam et al. 2013). All model spectra, as well as most of the data that were not available on WISEREP, were obtained with the help of the graph digitizer software, GraphClick.³

³ The full software is available at <http://www.arizona.edu/~davidb/graphclick/>

JTP would like to give special thanks to David Branch and J. Craig Wheeler for extensive discussions and valuable advice during the preparation of this manuscript. This work also benefitted from discussions with Rafaella Margutti, Maria Drout, Brian Friesen, Federica Bianco, and Isaac Shivvers.

REFERENCES

Aldering, G., Humphreys, R. M., & Richmond, M. 1994, AJ, 107, 662

Anderson, J. P., et al. 2014, MNRAS, 441, 671

Anupama, G. C., Sahu, D. K., Gurugubelli, U. K., Prabhu, T. P., Tominaga, N., Tanaka, M., & Nomoto, K. 2009, MNRAS, 392, 894

Anupama, G. C., Sahu, D. K., & Jose, J. 2005, A&A, 429, 667

Barbon, R., Benetti, S., Cappellaro, E., Patat, F., Turatto, M., & Iijima, T. 1995, A&AS, 110, 513

Baron, E., Branch, D., Hauschildt, P. H., Filippenko, A. V., & Kirshner, R. P. 1999, ApJ, 527, 739

Baron, E., Hauschildt, P. H., Branch, D., Wagner, R. M., Austin, S. J., Filippenko, A. V., & Matheson, T. 1993, ApJL, 416, L21

Baron, E., Hauschildt, P. H., & Mezzacappa, A. 1995, arXiv:astro-ph/9511081

Ben-Ami, S., et al. 2012, ApJL, 760, L33

Benetti, S., et al. 2004, MNRAS, 348, 261

—. 2011, MNRAS, 411, 2726

—. 2014, MNRAS, 441, 289

Bersten, M. C., et al. 2014, AJ, 148, 68

Blondin, S., Dessart, L., & Hillier, D. J. 2015, arXiv:1501.06583

Branch, D. 1972, A&A, 16, 247

Branch, D., Parrent, J., Troxel, M. A., Casebeer, D., Jeffery, D. J., Baron, E., Ketchum, W., & Hall, N. 2007, in American Institute of Physics Conference Series, Vol. 924, The Multicolored Landscape of Compact Objects and Their Explosive Origins, ed. T. di Salvo, G. L. Israel, L. Piersant, L. Burderi, G. Matt, A. Tornambe, & M. T. Menna, 342–349

Branch, D., et al. 2002, ApJ, 566, 1005

—. 2006, PASP, 118, 560

Burrows, A. 2013, Reviews of Modern Physics, 85, 245

Chatzopoulos, E., et al. 2011, ApJ, 729, 143

Childress, M. J., et al. 2013, ApJ, 770, 29

Clocchiatti, A., & Wheeler, J. C. 1997, in NATO Advanced Science Institutes (ASI) Series C, Vol. 486, NATO Advanced Science Institutes (ASI) Series C, ed. P. Ruiz-Lapuente, R. Canal, & J. Isern, 863

Clocchiatti, A., Wheeler, J. C., Brotherton, M. S., Cochran, A. L., Wills, D., Barker, E. S., & Turatto, M. 1996, ApJ, 462, 462

Cohen, J. G., Darling, J., & Porter, A. 1995, AJ, 110, 308

Corsi, A., et al. 2011, ApJ, 741, 76

D'Elia, V., et al. 2015, arXiv:1502.04883

Deng, J., Tominaga, N., Mazzali, P. A., Maeda, K., & Nomoto, K. 2005, ApJ, 624, 898

Deng, J. S., Qiu, Y. L., Hu, J. Y., Hatano, K., & Branch, D. 2000, ApJ, 540, 452

Dessart, L., Blondin, S., Hillier, D. J., & Khokhlov, A. 2014, MNRAS, 441, 532

Dessart, L., & Hillier, D. J. 2006, A&A, 447, 691

Dessart, L., Hillier, D. J., Li, C., & Woosley, S. 2012, MNRAS, 424, 2139

Dessart, L., Waldman, R., Livne, E., Hillier, D. J., & Blondin, S. 2013, MNRAS, 428, 3227

Doull, B. A., & Baron, E. 2011, PASP, 123, 765

Drout, M. R., et al. 2013, ApJ, 774, 58

Elmhamdi, A., Danziger, I. J., Branch, D., & Leibundgut, B. 2007, in American Institute of Physics Conference Series, Vol. 924, The Multicolored Landscape of Compact Objects and Their Explosive Origins, ed. T. di Salvo, G. L. Israel, L. Piersant, L. Burderi, G. Matt, A. Tornambe, & M. T. Menna, 277–284

Elmhamdi, A., Danziger, I. J., Branch, D., Leibundgut, B., Baron, E., & Kirshner, R. P. 2006, A&A, 450, 305

software.ch/graphclick/.

Elmhamdi, A., Danziger, I. J., Cappellaro, E., Della Valle, M., Gouffes, C., Phillips, M. M., & Turatto, M. 2004, A&A, 426, 963

Faran, T., et al. 2014, MNRAS, 445, 554

Filippenko, A. V. 1988, Proceedings of the Astronomical Society of Australia, 7, 540

—. 1997, ARA&A, 35, 309

Filippenko, A. V., Porter, A. C., & Sargent, W. L. W. 1990, AJ, 100, 1575

Folatelli, G., et al. 2006, ApJ, 641, 1039

Foley, R. J., et al. 2003, PASP, 115, 1220

—. 2009, AJ, 138, 376

Fox, O. D., et al. 2014, ApJ, 790, 17

Fryer, C. L., ed. 2004, Astrophysics and Space Science Library, Vol. 302, Stellar Collapse

Gal-Yam, A., Mazzali, P. A., Manulis, I., & Bishop, D. 2013, PASP, 125, 749

Gal-Yam, A., et al. 2009, Nature, 462, 624

Gall, E. E. E., et al. 2015, arXiv:1502.06034

Garnavich, P. M., et al. 2004, ApJ, 613, 1120

Gray, R. O., & Corbally, J. C. 2009, Stellar Spectral Classification

Hachinger, S., Mazzali, P. A., Taubenberger, S., Fink, M., Pakmor, R., Hillebrandt, W., & Seitenzahl, I. R. 2012, MNRAS, 427, 2057

Inserra, C., et al. 2013, ApJ, 770, 128

Iwamoto, K., Nomoto, K., Höflich, P., Yamaoka, H., Kumagai, S., & Shigeyama, T. 1994, ApJL, 437, L115

Iwamoto, K., et al. 1998, Nature, 395, 672

James, S., & Baron, E. 2010, ApJ, 718, 957

Jeffery, D. J., Branch, D., Filippenko, A. V., & Nomoto, K. 1991, ApJL, 377, L89

Jeffery, D. J., Leibundgut, B., Kirshner, R. P., Benetti, S., Branch, D., & Sonneborn, G. 1992, ApJ, 397, 304

Jerkstrand, A., Ergon, M., Smartt, S. J., Fransson, C., Sollerman, J., Taubenberger, S., Bersten, M., & Spyromilio, J. 2015, aap, 573, A12

Kasliwal, M. M., et al. 2010, ApJL, 723, L98

—. 2012, ApJ, 755, 161

Kerzendorf, W. E., & Sim, S. A. 2014, MNRAS, 440, 387

Lentz, E. J., Baron, E., Branch, D., & Hauschildt, P. H. 2001, ApJ, 557, 266

Lyman, J., Bersier, D., James, P., Mazzali, P., Eldridge, J., Fraser, M., & Pian, E. 2014, arXiv:1406.3667

Matheson, T., Filippenko, A. V., Li, W., Leonard, D. C., & Shields, J. C. 2001, AJ, 121, 1648

Maund, J. R., Smartt, S. J., Kudritzki, R. P., Podsiadlowski, P., & Gilmore, G. F. 2004, Nature, 427, 129

Maund, J. R., et al. 2013, MNRAS, 433, L20

Mazzali, P. A., Iwamoto, K., & Nomoto, K. 2000, ApJ, 545, 407

Mazzali, P. A., Walker, E. S., Pian, E., Tanaka, M., Corsi, A., Hattori, T., & Gal-Yam, A. 2013, MNRAS, 432, 2463

Mazzali, P. A., et al. 2003, ApJL, 599, L95

—. 2006, ApJ, 645, 1323

—. 2014, MNRAS, 439, 1959

McLaughlin, D. B. 1961, AJ, 66, 291

Milisavljevic, D., et al. 2013, ApJ, 767, 71

—. 2015, ApJ, 799, 51

Minkowski, R. 1941, PASP, 53, 224

Modjaz, M., et al. 2009, ApJ, 702, 226

—. 2014, AJ, 147, 99

Moriya, T., Tominaga, N., Tanaka, M., Maeda, K., & Nomoto, K. 2010, ApJL, 717, L83

Nicholl, M., et al. 2014, MNRAS, 444, 2096

—. 2015, arXiv:1503.03310

Nomoto, K., Iwamoto, K., Suzuki, T., Pols, O. R., Yamaoka, H., Hashimoto, M., Hofflich, P., & van den Heuvel, E. P. J. 1996, in IAU Symposium, Vol. 165, Compact Stars in Binaries, ed. J. van Paradijs, E. P. J. van den Heuvel, & E. Kuulkers, 119

Nomoto, K., et al. 2000, in American Institute of Physics Conference Series, Vol. 526, Gamma-ray Bursts, 5th Huntsville Symposium, ed. R. M. Kippen, R. S. Mallozzi, & G. J. Fishman, 622–627

Parrent, J., et al. 2007, PASP, 119, 135

Parrent, J. T. 2014, arXiv:1412.7163

Parrent, J. T., et al. 2012, ApJL, 752, L26

Pastorello, A., et al. 2006, MNRAS, 370, 1752

Patat, F., Benetti, S., Cappellaro, E., Danziger, I. J., della Valle, M., Mazzali, P. A., & Turatto, M. 1996, MNRAS, 278, 111

Patat, F., et al. 2001, ApJ, 555, 900

Pejcha, O., & Prieto, J. L. 2015, arXiv:1501.06573

Pereira, R., et al. 2013, A&A, 554, A27

Poznanski, D., et al. 2010, Science, 327, 58

Pun, C. S. J., et al. 1995, ApJS, 99, 223

Richardson, D., Thomas, R. C., Casebeer, D., Blankenship, Z., Ratowt, S., Baron, E., & Branch, D. 2001, in Bulletin of the American Astronomical Society, Vol. 33, American Astronomical Society Meeting Abstracts, 1428

Sanders, N. E., et al. 2014, arXiv:1404.2004

Sauer, D. N., Hoffmann, T. L., & Pauldrach, A. W. A. 2006, A&A, 459, 229

Smartt, S. J. 2009, ARAA, 47, 63

—. 2015, arXiv:1504.02635

Smith, N., et al. 2007, ApJ, 666, 1116

Soderberg, A. M., et al. 2008a, Nature, 453, 469

—. 2008b, Nature, 453, 469

Stathakis, R. A., et al. 2000, MNRAS, 314, 807

Sullivan, M., et al. 2011, ApJ, 732, 118

Taubenberger, S., et al. 2006, MNRAS, 371, 1459

—. 2011, MNRAS, 412, 2735

Valenti, S., et al. 2008, ApJL, 673, L155

—. 2011, MNRAS, 416, 3138

—. 2014, MNRAS, 437, 1519

van Dyk, S. D., Hamuy, M., & Filippenko, A. V. 1996, AJ, 111, 2017

Van Dyk, S. D., et al. 2011, ApJL, 741, L28

Walker, E. S., et al. 2014, MNRAS, 442, 2768

Wheeler, J. C., Harkness, R. P., Clocchiatti, A., Benetti, S., Brotherton, M. S., Depoy, D. L., & Elias, J. 1994, ApJL, 436, L135

Wheeler, J. C., Harkness, R. P., Khokhlov, A. M., & Hoeflich, P. 1995, Physics Reports, 256, 211

Yaron, O., & Gal-Yam, A. 2012, PASP, 124, 668

Yoon, S.-C. 2015, PASA, 32, 15

Yoshida, T., & Umeda, H. 2011, MNRAS, 412, L78